Inorganic Chemistry

ARTICLE

pubs.acs.org/IC

Influence of the Electronic Characteristics of N-Donor Ligands in the Excited State of Heteronuclear Gold(I)−Copper(I) Systems

José M. López-de-Luzuriaga,* Miguel Monge, M. Elena Olmos, David Pascual, and María Rodríguez-Castillo

Departamento de Química, Universidad de La Rioja, Grupo de Síntesis Química de La Rioja, UA-CSIC, Complejo Científico-Tecnológico, 26004-Logroño, Spain

Supporting Information

ABSTRACT: By reaction of the heterometallic gold−silver complexes $[\{AuAg(C_6F_5)_2(N{\equiv}C{-}Me)\}_2]_n$ or $[\{AuAg(C_6Cl_5)_2(N{\equiv}C{-}Me)\}_2]_n$ and CuCl in the presence of pyrimidine and different nitrile ligands (acetonitrile, benzonitrile, and cinnamonitrile), the heteronuclear complexes $\{[Au(C_6X_5)_2][Cu(L)(\mu_2\text{-}C_4H_4N_2)]\}_n$ (X = F and L = N≡C−Me (**1**), L = N≡C−Ph (**2**) or N≡C−CH═CH−Ph (**3**); X = Cl and L = N≡C−Me (**4**), N≡C−Ph (**5**), N≡C−CH═CH−Ph (**6**)) have been prepared. The crystal structures of complexes $\{[Au(C_6X_5)_2][Cu(L)(\mu_2\text{-}C_4H_4N_2)]\}_n$ (X = F; L = N≡C−CH═CH−Ph (**3**), X = Cl; L = N≡C−Ph (**5**)) have been determined by X-ray diffraction studies. The crystal structures of both complexes consists of polymeric chains formed by the repetition of $[Au(C_6X_5)_2][Cu(L)(\mu_2\text{-}C_4H_4N_2)]$ units through copper−pyrimidine bonds. Complexes **1**, **2**, **4**, and **5** are brightly luminescent in the solid state at room temperature and at 77 K with lifetimes in the microseconds range. These compounds are also luminescent in solution, displaying different photophysical behaviors depending on the donor characteristics of the solvents used. The distortion in the excited state allows an associative attack by donor solvents quenching one of the emitting excited states. DFT optimizations of the ground (S_0) and lowest triplet excited state (T_1) display the structure distortion of the complexes upon electronic excitation. The molecular orbitals involved in the electronic transitions responsible for the phosphorescence in the case of the complexes **1**, **2**, **4**, and **5** are related to metal (gold−copper) to ligand (pyrimidine) charge transfer transitions, while in the case of the nonluminescent complexes **3** and **6**, the nonradiative electronic transition arises from metal (gold−copper) to ligand (cinnamonitrile) charge transfer transitions.

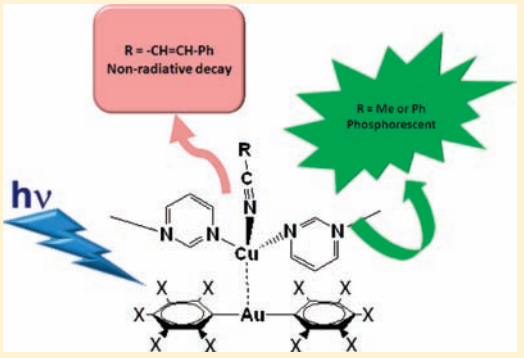

INTRODUCTION

The chemistry of gold−heterometal complexes bearing unsupported closed-shell metallophilic interactions has grown rapidly in recent years as a result of the increasing interest in the intrinsic nature of these interactions[1] and the commonly associated photoluminescent properties.[2] Many studies have demonstrated that the presence of unsupported Au···M metallophilic interactions (M = Ag(I),[3] Tl(I),[4] Bi(III),[5] Hg(II),[6] Hg(0),[7] or Cu(I)[8]) plays a more than significant role in the formation of the supramolecular arrangements found in the solid state. Thus, a rational molecular design of each heterometallic molecular component has led to a wide variety of structural organizations going from discrete dinuclear[9] to 1D,[10] 2D,[11] or 3D-polymeric[12] structural dispositions. Also, a large number of these complexes display interesting and different emissive properties that depend on the type of closed-shell metals, strength of the interactions, metal coordination environments, or even the types of ligands connected to the metals. The systematic changes of one or several of these parameters have given rise to different classes of luminescent compounds, going from fluorescent to phosphorescent emitters or from high energy (blue) to low energy (red) emissions, in which the mechanism responsible for the emissions could arise from metal-centered transitions (MC) or charge transfer transitions (CT). In any case, the presence of the metallophilic interactions in the complexes clearly influences the photoluminescent emissions.[2]

One fundamental help for this rational design that allows the tuning of the photoluminescence is the use of theoretical calculations for the interpretation of the mechanisms responsible for the emissions and their comparisons with the experimental results. In this sense, the earliest calculations were carried out, and still are, using the TD-DFT formalism[13] that permits the prediction of the theoretical electronic transitions that could be responsible for the emissive properties. This TD-DFT approach is very useful from a time-consuming point of view and provides interesting information of the electronic excitations based on the ground state structural disposition. More recently, the excited state optimization of gold-containing compounds has been studied by several groups, which allows for the analysis of the structural distortions of the excited state associated with the electronic transition and the singly occupied molecular orbitals

Received: December 22, 2010
Published: June 30, 2011

Scheme 1

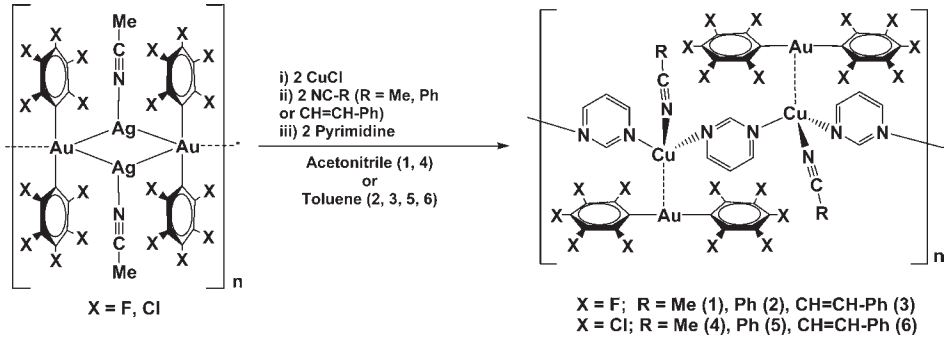

from which the emissions are produced. With this approach, we have characterized, for example, the Jahn−Teller distortion of the lowest triplet excited state of a dinuclear Au(I) complex with distibine ligands[14] or a distortion beyond a T-shape for a Au−Tl complex.[9] These results can be interpreted when a deep photophysical study is carried out at the same time.

We have used in recent years a very productive strategy for the synthesis of heterometallic Au−M complexes displaying Au···M interactions in the solid state and even in solution. This method consists of an acid−base reaction between a $[Au(C_6X_5)_2]^-$ (X = F, Cl) Lewis basis and Ag(I), Tl(I), or Bi(III) acid salts.[3−5] We have also described that for the specific case of the heterometallic Au(I)−Cu(I) complexes the acid−base reaction does not occur under similar conditions, and instead a transmetalation reaction of the corresponding heterometallic Au−Ag complex $[\{AuAg(C_6F_5)_2(N{\equiv}C{-}Me)\}_2]_n$ with CuCl in the presence of different types of N-donor ligands gives rise to similar aurate-heterometal complexes bearing unsupported Au(I)···Cu(I) intermetallic interactions. Thus, we have recently reported the first unsupported Au(I)···Cu(I) interactions between bis(pentafluorophenyl)aurate(I) units and Cu(I) acid sites bonded to pyrimidine and/or nitrile ligands.[8,15,16] In the first case, we observed a clear influence of the aromatic pyrimidine ligand on the photoluminescent properties, a metal−metal-to-ligand charge transfer (MMLCT) being the origin of the emission in the solid state. By contrast, the study of Au(I)−Cu(I) nitrile compounds shows that the presence of aurophilic interactions in the solid state is a prerequisite for the observation of a luminescent emission.

Taking all of these facts into account, we go on with the study of this heteronuclear Au(I)−Cu(I) chemistry in order to exercise control over their luminescent properties such as, for instance, emission energy tuning or on−off switching of the emissive properties by slight molecular changes. In this context, according to our experience, the use of different perhalophenyl ligands bonded to Au(I) such as C_6F_5 or C_6Cl_5 or different nitrile ligands bonded to Cu(I) can be used for these purposes. For example, the change of the perhalophenyl group bonded to gold(I) permits the modification of the basicity of the aurate units, while the change of the R substituent of the nitrile ligands (N≡C−R; R = Me or Ph) can also modulate the accepting abilities of these ligands. These changes would, in principle, permit a tuning of the emission energies since the luminescent electronic transitions are very sensitive to the electron density distribution in the compounds, especially when charge transfer transitions are the origin of the emissions. Moreover, it is also known that nitrile ligands bearing double bonds such as cinnamonitrile can act as electron acceptors in the quench via nonradiative pathways of luminescent molecules.[17] This type of nitrile ligand could be used as a molecular tool for the selective luminescent deactivation of heteropolynuclear Au(I)−Cu(I) compounds.

Herein, we report the synthesis and characterization of complexes $\{[Au(C_6X_5)_2][Cu(L)(\mu_2\text{-}C_4H_4N_2)]\}_n$ (X = F and L = N≡C−Ph (**2**) or N≡C−CH=CH−Ph (**3**); X = Cl and L = N≡C−Me (**4**), N≡C−Ph (**5**), or N≡C−CH=CH−Ph (**6**)). We have carried out a deep study of their photophysical properties and a theoretical interpretation of the excited state properties via DFT calculations. In a first step, we have analyzed the different factors that change the emission energy of these compounds, the change of the perhalophenyl groups bonded to gold(I) or the use of different nitrile ligands such as acetonitrile and benzonitrile, including a comparison with the previously reported complex $\{[Au(C_6F_5)_2][Cu(N{\equiv}C{-}Me)(\mu_2\text{-}C_4H_4N_2)]\}_n$ (**1**). We have also analyzed the different photophysical properties induced when the cinnamonitrile ligand is bonded to Cu(I). Finally, the DFT optimization of the ground and lowest triplet excited states of model systems of these Au−Cu complexes allows us to explain the different photophysical behavior observed experimentally.

RESULTS AND DISCUSSION

Synthesis and Structural Characterization. The use of heterometallic gold−silver complexes $[\{AuAg(C_6X_5)_2(N{\equiv}C{-}Me)\}_2]_n$ (X = F, Cl) as starting materials permits the synthesis of a variety of heterometallic gold−copper species through a transmetalation reaction, due to the propensity of Cu(I) to form stable derivatives in the presence of nitrile ligands. Thus, treatment of these Au−Ag compounds with CuCl, using acetonitrile as a solvent and in the presence of a pyrimidine ligand in a 1:1:1 gold/copper/pyrimidine molar ratio, leads to a transmetalation reaction giving rise to complexes of stoichiometry $\{[Au(C_6X_5)_2][Cu(N{\equiv}C{-}Me)(\mu_2\text{-}C_4H_4N_2)]\}_n$ (X = F (**1**),[8] Cl (**4**)). Complexes $[\{AuAg(C_6X_5)_2(N{\equiv}C{-}Me)\}_2]_n$ (X = F, Cl) can also be used as precursors for the synthesis of new Au−Cu complexes bearing pyrimidine ligands and other nitrile ligands such as benzonitrile and cinnamonitrile. Thus, the corresponding Au−Cu precursors were prepared when complexes $[\{AuAg(C_6X_5)_2(N{\equiv}C{-}Me)\}_2]_n$ were reacted with CuCl in acetonitrile. Benzonitrile or cinnamonitrile and pyrimidine in a 1:1:1 (Cu/nitrile/pyrimidine) molar ratio were added in toluene. The replacement of the acetonitrile ligand with the added nitrile and the coordination of pyrimidine to Cu(I) took place, leading to complexes $\{[Au(C_6X_5)_2][Cu(L)(\mu_2\text{-}C_4H_4N_2)]\}_n$ (X = F and L = N≡C−Ph (**2**) or N≡C−CH=CH−Ph (**3**); X = Cl and L = N≡C−Ph (**5**) or N≡C−CH=CH−Ph (**6**); see Scheme 1). The ^{1}H NMR spectra of complexes **2**−**6** display signals

dx.doi.org/10.1021/ic102550z |Inorg. Chem. 2011, 50, 6910–6921

Table 1. Data Collection and Structure Refinement Details for Complexes 3 and 5

compound	3	5
chemical formula	$C_{25}H_{11}AuCuF_{10}N_3$	$C_{23}H_9AuCuCl_{10}N_3$
cryst habit	colorless prism	yellow prism
cryst size/mm	0.12 × 0.11 × 0.08	0.1 × 0.05 × 0.05
cryst syst	monoclinic	monoclinic
space group	$P2_1/c$	$C2/c$
a/Å	10.0747(3)	19.2579(8)
b/Å	23.8833(6)	10.2493(4)
c/Å	11.3984(4)	28.8366(11)
β/deg	116.640(1)	105.266(2)
U/Å^3	2451.49(13)	5490.9(4)
Z	4	8
D_c /g cm^{-3}	2.178	2.280
M	803.87	942.34
$F(000)$	1520	3568
T/°C	−173	−153
$2\theta_{max}$/deg	55	56
μ(Mo Kα)/mm^{-1}	6.942	7.108
no. reflns measured	40990	20160
no. unique reflns	5602	6193
R_{int}	0.0811	0.0793
R^a ($I > 2\sigma(I)$)	0.0319	0.0461
wR^b (F^2, all reflns)	0.0642	0.0814
no. params	361	343
no. restraints	113	104
S^c	1.038	1.020
max. $\Delta\rho$/eÅ^{-3}	2.234	2.341

$^a R(F) = \sum ||F_o| - |F_c|| / \sum |F_o|$. $^b wR(F^2) = [\sum\{w(F_o^2 - F_c^2)^2\} / \sum\{w(F_o^2)^2\}]^{0.5}$; $w^{-1} = \sigma^2(F_o^2) + (aP)^2 + bP$, where $P = [F_o^2 + 2F_c^2]/3$ and a and b are constants adjusted by the program. $^c S = [\sum\{w(F_o^2 - F_c^2)^2\} / (n - p)]^{0.5}$, where n is the number of data and p is the number of parameters

corresponding to the nitrile and pyrimidine ligands (see the Experimental Section). The chemical shifts for the acetonitrile, benzonitrile, and cinnamonitrile species are similar to those of the free nitrile ligands, probably due to dissociation processes in solution. However, the chemical shifts corresponding to the aromatic protons of the pyrimidine ligand are different from the free ones, indicating the coordination of these ligands to the copper(I) centers in solution. Complexes **2** and **3** display similar ^{19}F NMR spectra, also similar to those of the precursor complex $NBu_4[Au(C_6F_5)_2]$, showing signals corresponding to the C_6F_5 groups bonded to Au(I) in the $[Au(C_6F_5)_2]^-$ units at −114.8 (F_o), −161.6 (F_p), and −162.8 (F_m) ppm, suggesting the rupture of the Au···Cu metallophilic interaction in solution. The IR spectra of **2** and **3** in Nujol mulls show absorptions arising from $[Au(C_6F_5)_2]^-$ groups at 1499−1502, 955−958, and 785 cm^{-1}. On the other hand, complexes **4**−**6** show the corresponding absorptions in the ranges 833−835 and 609−612 cm^{-1}, according to the presence of $[Au(C_6Cl_5)_2]^-$ units. In all of these complexes, the absorptions due to the organic ligands coordinated to the Cu(I) centers can be assigned. These bands appear at significantly different energies from the absorptions of the uncoordinated organic ligands. For example, complexes **2** and **5** display bands at 2240 and 2245 cm^{-1}, respectively, due to the ν(C≡N) stretching vibration, while, in the free ligand, this band

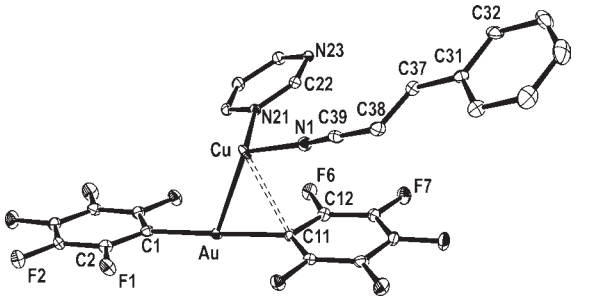

Figure 1. Crystal structure of complex **3**.

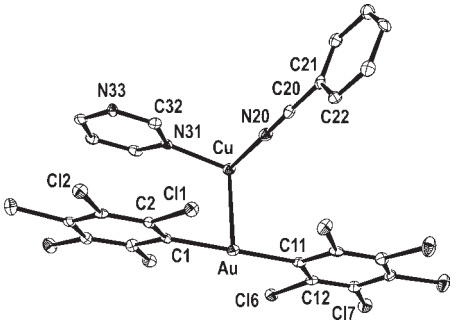

Figure 2. Crystal structure of complex **5**.

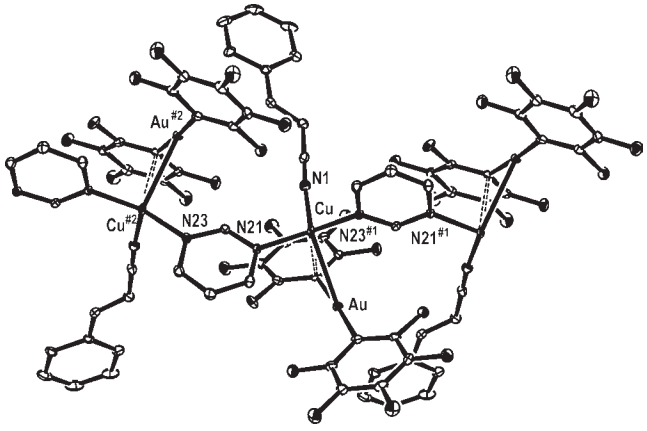

Figure 3. One-dimensional structure of complex **3**.

appears at 2226 cm^{-1}. Complexes **3** and **6** display the corresponding ν(C≡N) stretching vibration at 2236 and 2228 cm^{-1}, respectively, while this absorption appears at 2218 cm^{-1} in the case of the free ligand. IR spectrum for complex **4** displays, again, a shift in the ν(C≡N) stretching vibration compared with the free acetonitrile, appearing at 2273 and 2253 cm^{-1}, respectively. The same happens with the pyrimidine ligand. In all complexes, the signals corresponding to the ν(C=N) stretching vibrations arising from the pyrimidine ligand are shifted. They appear in the range 1559−1633 cm^{-1}, as the free ligand displays absortions bands around 1571 cm^{-1}.

Crystal Structures. Crystal structures of complexes **3** and **5** were determined using X-ray diffraction from single crystals obtained through the slow diffusion of *n*-hexane into a solution of the complex in dichloromethane. Both complexes correspond to the general formula $\{[Au(C_6X_5)_2][Cu(N{\equiv}C{-}R)(\mu_2\text{-}C_4H_4N_2)]\}_n$ and crystallize in the monoclinic system, although in different space groups

dx.doi.org/10.1021/ic102550z |*Inorg. Chem.* 2011, 50, 6910–6921

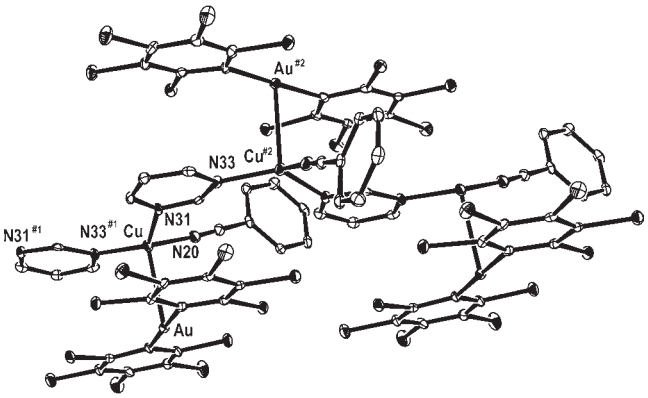

Figure 4. One-dimensional structure of complex **5**.

Table 2. Selected Bond Lengths [Å] and Angles [deg] for Complex 3[a]

Au−C(1)	2.047(5)	Cu−N(21)	1.997(4)
Au−C(11)	2.057(4)	Cu−N(1)	2.000(4)
Au−Cu	2.7614(6)	Cu−N(23)#1	2.001(4)
C(1)−Au−C(11)	176.58(17)	N(21)−Cu−Au	94.69(10)
N(21)−Cu−N(1)	109.71(15)	N(1)−Cu−Au	128.67(12)
N(21)−Cu−N(23)#1	128.94(14)	N(23)#1−Cu−Au	95.52(10)
N(1)−Cu−N(23)#1	101.99(15)		

[a] Symmetry transformations used to generate equivalent atoms: (#1) x, $-y + 1/2$, $z - 1/2$; (#2) x, $-y + 1/2$, $z + 1/2$.

Table 3. Selected Bond Lengths [Å] and Angles [deg] for Complex 5[a]

Au−C(11)	2.037(6)	Cu−N(20)	1.969(5)
Au−C(1)	2.038(6)	Cu−N(33)#1	1.993(5)
Au−Cu	2.7255(8)	Cu−N(31)	2.043(5)
C(11)−Au−C(1)	179.0(2)	N(20)−Cu−Au	96.94(16)
N(20)−Cu−N(33)#1	114.7(2)	N(33)#1−Cu−Au	97.64(14)
N(20)−Cu−N(31)	106.4(2)	N(31)−Cu−Au	110.20(13)
N(33)#1−Cu−N(31)	126.5(2)		

[a] Symmetry transformations used to generate equivalent atoms: #1 $-x + 3/2$, $y - 1/2$, $-z + 3/2$.

(see Table 1). Both crystal structures consist of polymeric chains formed by the repetition of heterodinuclear units (Figures 1 and 2) that are linked through the bridging pyrimidine ligands, which are bonded to the copper(I) centers of adjacent Au/Cu fragments through the nitrogen atoms (Figures 3 and 4).

The Cu−Npyr bond distances, of 1.997(4) and 2.001(4) Å in **3** and 1.993(5) and 2.043(5) Å in **5** (see Tables 2 and 3), are all nearly equal to those found in the isostructural acetonitrile derivative $\{[Au(C_6F_5)_2][Cu(N{\equiv}C{-}Me)(\mu_2\text{-}C_4H_4N_2)]\}_n$ (**1**) previously described by us (Cu−Npyr: 1.987(3), 2.003(4) Å).[8] The Cu−N bond distance to the nitrile is very similar to those of the pyrimidine ligands, displaying values of 2.000(4) Å in **3** and 1.969(5) Å in **5**, which are slightly longer than in complexes $\{[Au(C_6F_5)_2][Cu(N{\equiv}C{-}CH{=}CHPh)_2]\}_n$ (1.866(3) and 1.871(3) Å)[16] and $\{[Au(C_6F_5)_2][Cu(N{\equiv}C{-}Ph)_2]\}_2$ (1.869(8)−1.877(8) Å).[16] These distances lie within the range of Cu−N≡C−R lengths found in the crystal structures of the previously reported related compounds $\{[Au(C_6F_5)_2][Cu(N{\equiv}C{-}Me)(\mu_2\text{-}C_4H_4N_2)]\}_n$,[8] $[\{AuCu(C_6F_5)_2(N{\equiv}C{-}Me)\}_2]_n$,[15] and $\{[Au(C_6F_5)_2][Cu(N{\equiv}C{-}R)_2]\}_x$ (x = 1 and R = Me, CH=CHPh; x = 2 and R = Ph)[16] or $[Au(C_6F_5)_2][Cu(N{\equiv}C{-}Cy{-}C{\equiv}N)_2]\cdot CH_2Cl_2$,[18] which vary from 1.866(3) to 2.048(4) Å. The $[Au(C_6F_5)_2]^-$ units can be seen as metalloligands that complete the distorted tetrahedral environment of the copper centers via an unsupported Au···Cu bonding interaction of 2.7614(6) (**3**) or 2.7255(8) Å (**5**). These values are again slightly longer than in the related nitrile complexes $\{[Au(C_6F_5)_2][Cu(N{\equiv}C{-}CH{=}CHPh)_2]\}$ (1.866(3) and 1.871(3) Å)[16] and $\{[Au(C_6F_5)_2][Cu(N{\equiv}C{-}Ph)_2]\}_2$ (1.869(8)−1.877(8) Å;[16] 2.6727(4) Å and 2.6163(12) and 2.6092(12) Å, respectively) and are intermediate between the Au−Cu separations observed in $\{[Au(C_6F_5)_2][Cu(N{\equiv}C{-}Me)(\mu_2\text{-}C_4H_4N_2)]\}_n$ (2.8216(6) Å),[8] $[\{AuCu(C_6F_5)_2(N{\equiv}C{-}Me)\}_2]_n$, or $\{[Au(C_6F_5)_2][Cu(N{\equiv}C{-}R)_2]\}_x$ (x = 1 and R = Me, CH=CHPh; x = 2 and R = Ph; 2.5741(16)−2.6727(4) Å)[15,16] and in some Au/Cu clusters (2.584, 2.589).[19,20]

The gold atoms can be considered tricoordinate, as they bind two pentahalophenyl rings (displaying typical Au−C bond lengths of 2.047(5) and 2.057(4) Å in **3** and 2.037(6) and 2.038(6) Å in **5**) and maintain an unsupported short interaction with a copper center. The main difference between both structures is the presence of Cu···C_{ipso} interactions of 2.698 Å in **3** (see Figure 1), which are absent in the crystal structure of complex **5** (see Figure 3). Such contacts are responsible for the distortion of the planar T-frame environment for the gold atoms in **3**, since they make one of the C−Au−Cu units narrower (66.26°) than the other (114.51°), while in **5**, they both are close to 90° (96.69 and 83.93°). It is worth noting that all of the related complexes previously reported, $\{[Au(C_6F_5)_2][Cu(N{\equiv}C{-}Me)(\mu_2\text{-}C_4H_4N_2)]\}_n$,[8] $[\{AuCu(C_6F_5)_2(N{\equiv}C{-}Me)\}_2]_n$,[15] and $\{[Au(C_6F_5)_2][Cu(N{\equiv}C{-}R)_2]\}_x$ (x = 1 and R = Me, CH=CHPh; x = 2 and R = Ph)[16] or $[Cu(N{\equiv}C{-}Cy{-}C{\equiv}N)_2][Au(C_6F_5)_2]\cdot CH_2Cl_2$,[18] also display such Cu···C_{ipso} contacts, so complex **5** is the only case in which they are not present.

Finally, the crystal structure of **5** displays a $\pi-\pi$ interaction between one of the pentachlorophenyl groups bonded to gold and the aromatic ring of one of the pyrimidine ligands (with a distance between the centroids of the rings of 3.317 Å), while in the case of complex **3**, such interactions between the rings are not observed.

Photophysical Studies. In spite of the similar structures found (see above), the luminescent properties of the complexes are different when they are irradiated with UV light, in the solid state as well as in solution, and these differences, as we will show in the next paragraphs, depend on the nitrile ligands bonded to the copper centers or the solvents used in the measurements, respectively.

Complexes $\{[Au(C_6F_5)_2][Cu(L)(\mu_2\text{-}C_4H_4N_2)]\}_n$ (L = N≡C−Me, **1**; N≡C−Ph, **2**; N≡C−CH=CH−Ph, **3**) display similar features in their UV−vis spectra (see Table 4). Thus, in all cases, they show absorptions at 225, 237, and 260 nm whose positions and intensities are similar to those found in the precursor $NBu_4[Au(C_6F_5)_2]$ and, consequently, are assigned to the same origin, i.e., transitions located in the pentafluorphenyl rings, probably involving π and π^* orbitals. In addition, complexes **1** and **2** show absorptions of less intensity at 290 and 295 nm (542 $mol^{-1}\,L\,cm^{-1}$) (observed at a higher concentration of 5×10^{-4} M), energy which is similar to the less energetic band that appears in the spectrum of the pyrimidine ligand, and therefore, we propose a similar origin. In complex **2**, the absorption at 277 nm is assigned to the

dx.doi.org/10.1021/ic102550z |Inorg. Chem. 2011, 50, 6910–6921

Table 4. Spectroscopic and Photophysical Properties of Complexes 1−6

complex	medium (T [K])	λ_{abs}[nm] (ε [mol^{-1} L cm^{-1}])[b]	λ_{em} (λ_{exc}) [nm]/τ (μs)
{[Au(C_6F_5)$_2$][Cu(N≡C−Me)(μ_2-$C_4H_4N_2$)]}$_n$ (**1**)[a]	CH_3CN (298)	211 (24500), 235 (22500), 260 (7000), 290 (232)	365 (290)
	CH_2Cl_2 (298)		394 (263), 530 (365)
	solid (RT)		525 (390)/10.3
	solid (77)		529 (371)
{[Au(C_6F_5)$_2$][Cu(N≡C−Ph)(μ_2-$C_4H_4N_2$)]}$_n$ (**2**)	CH_3CN (298)	225 (37894), 237 (sh)[c], 260 (8926), 277 (1700), 295 (542)[d]	352 (290)
	CH_2Cl_2 (298)		340 (290), 525 (365)
	solid (RT)		522 (370)/8.6
	solid (77)		529 (370)
{[Au(C_6F_5)$_2$][Cu(N≡C−CH=CH−Ph)(μ_2-$C_4H_4N_2$)]}$_n$ (**3**)	CH_3CN (298)	222 (37600), 237 (28296), 263 (26560)	337 (290)
	CH_2Cl_2 (298)		343 (290)
	solid (RT)		
	solid (77)		
{[Au(C_6Cl_5)$_2$][Cu(N≡C−Me)(μ_2-$C_4H_4N_2$)]}$_n$ (**4**)	CH_3CN (298)	219 (84380), 274 (13800), 299 (3970)	370 (280)
	CH_2Cl_2 (298)		420 (290), 597 (380)
	solid (RT)		526 (366)/25.0
	solid (77)		531 (370)
{[Au(C_6Cl_5)$_2$][Cu(N≡C−Ph)(μ_2-$C_4H_4N_2$)]}$_n$ (**5**)	CH_3CN (298)	219 (111230), 274 (17400), 299 (5000)	367 (290)
	CH_2Cl_2 (298)		424 (280), 598 (380)
	solid (RT)		590 (370)/10.0
	solid (77)		615 (400)
{[Au(C_6Cl_5)$_2$][Cu(N≡C−CH=CH−Ph)(μ_2-$C_4H_4N_2$)]}$_n$ (**6**)	CH_3CN (298)	222 (97180), 272 (32990), 299 (7620)	364 (290)
	CH_2Cl_2 (298)		396 (280)
	solid (RT)		
	solid (77)		

[a] See ref 8. [b] 4.3 × 10^{-5} M (**1**), 5.0 × 10^{-5} M (**2**, **3**), and 10^{-5} M (**4**−**6**) in acetonitrile [c] sh = shoulder. [d] 5.0 × 10^{-4} M.

benzonitrile ligand. In the case of complex **3**, the band due to the pyrimidine ligand is probably masked by the cinnamonitrile ligand, whose band edge is placed at 295 nm.

For complexes {[Au(C_6Cl_5)$_2$][Cu(L)(μ_2-$C_4H_4N_2$)]}$_n$ (L = N≡C−Me, **4**; N≡C−Ph, **5**; N≡C−CH=CH−Ph, **6**), we observe a similar situation as in the previous ones with the presence of absorption bands at *ca.* 220 and 272 nm in the three complexes, due to transitions between π and π^* orbitals in the pentachlorophenyl rings, since they also appear in the precursor NBu_4[Au(C_6Cl_5)$_2$], and at 299 nm, assigned to the pyrimidine ligand. In the case of complex **6**, the intensity of the band at 272 nm is higher than in the other two complexes (ε = 13 800 (**4**), 17 400 (**5**), and 32 990 (**6**) M^{-1} cm^{-1}), but this fact is probably due to the overlapping of this band with that due to the cinnamonitrile ligand that appears for the free nitrile at 273 nm (Figure 5).

Interestingly, we do not observe any transition assigned to the gold−copper interaction that appears in the solid state structure of the complexes in any case, neither do we observe shifts of the positions of the bands, not even when we increase considerably the concentration of the samples.

The similarity in the optical behavior found in the absorption spectra for the six complexes was not seen in the emission spectra in the solid state, depending on the nitrile ligand, or in solution, depending on the solvent. Thus, while complexes **1**, **2**, **4**, and **5** are strongly luminescent in the solid state at room temperature with emissions at 525, 522, 526, and 590 nm, shifting to 529, 529, 531, and 615 nm at 77 K, respectively, complexes **3** and **6** do not show luminescence at both temperatures (Figure 6). The lifetime

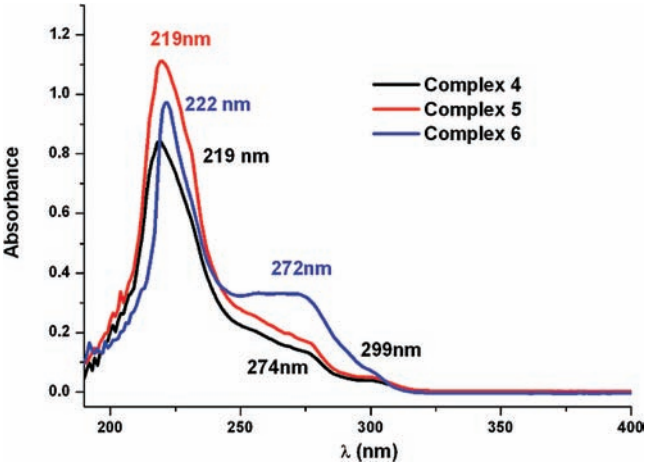

Figure 5. UV−vis spectra for complexes **4**−**6** in 10^{-5} M acetonitrile solutions.

measurements in the solid state at room temperature give in all cases values in the range of microseconds. These values, together with the large Stokes shifts, suggest phosphorescent processes; nevertheless, the large spin−orbit coupling expected in these materials does not allow for making a definitive assignment.

In principle, it is very surprising that complexes displaying such similar structures with similar structural parameters show different optical behaviors. These differences cannot be related to the

dx.doi.org/10.1021/ic102550z |*Inorg. Chem.* 2011, 50, 6910–6921

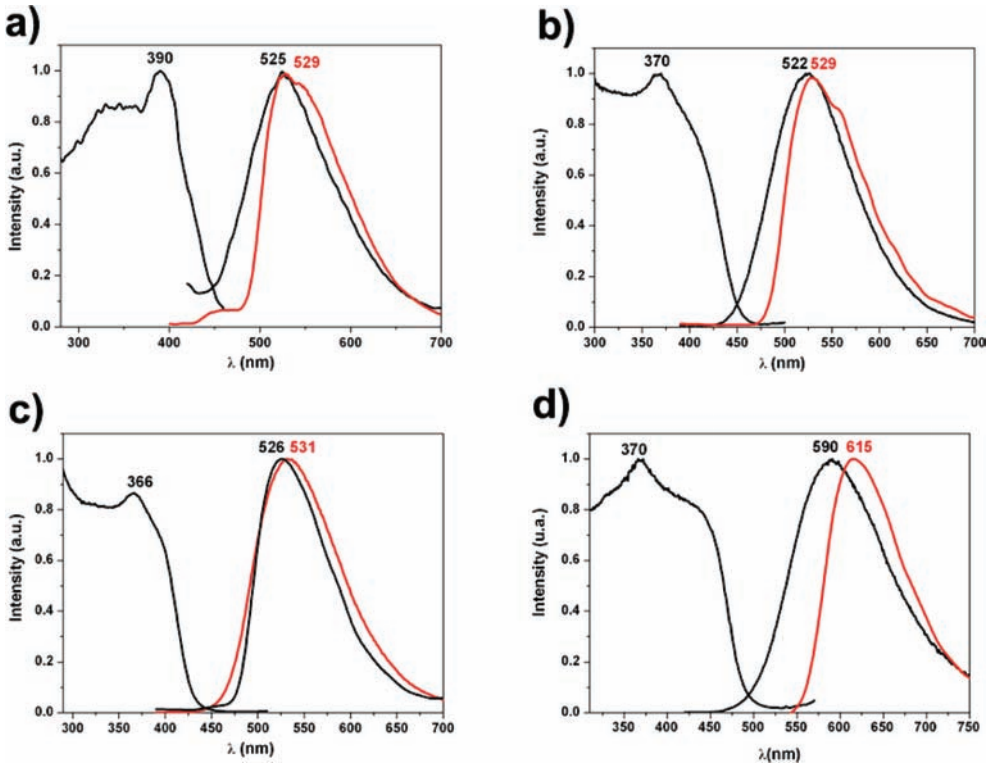

Figure 6. Normalized excitation and emission spectra in the solid state at RT (black) and emission at 77 K (red) for complexes **1** (a), **2** (b), **4** (c), and **5** (d).

different perhalophenyl group present in each complex, since complex **1** and complex **3** have both pentafluorophenyl ligands and the former show luminescence and the latter does not. By contrast, complex **5** contains pentachlorophenyl groups, and it shows luminescence. Neither the presence or absence of $\pi-\pi$ interactions between these perhalophenyl groups and the pyrimidine ligands can be considered as the origin of this different behavior, since complex **5** displays this type of interaction in the solid state structure (see above) and it is luminescent, while in the case of complexes **1** and **3**, without $\pi-\pi$ interactions between the rings, the former displays an emission, but the latter does not.

The complexes that do not show luminescence in the solid state have in common the presence of the cinnamonitrile ligand; consequently, it is reasonable to think that the absence of the emission in complexes **3** and **6** is related with this nitrile. This fact has been further confirmed by the DFT calculations carried out (see below).

Another interesting feature of these complexes is the optical behavior in solution. All of them display luminescence, but the energy of the emissions depends on the solvent characteristics. For instance, complexes **1**−**6** display one high energy emission in acetonitrile solutions (5×10^{-4} M), appearing at 365 (exc 290), **1**; 352 (exc. 290), **2**; 343 (exc. 290), **3**; 370 (exc. 280), **4**; 367 (exc. 290), **5**; and 395 nm (exc. 280 nm), **6**, one in noncoordinant solvents such as dichloromethane (5×10^{-4} M) for complexes **3** and **6** at 337 (exc. 290) and 360 nm (exc. 290 nm), respectively, but two independent emissions in dichloromethane for complexes **1** (em. 394, exc. 263; em 530, exc. 369), **2** (em. 340, exc. 290; em. 525, exc. 365), **4** (em. 420, exc. 290; em. 597, exc. 380), and **5** (em. 424, exc. 280; em. 598, exc. 380). In summary, in all of the complexes, only one high energy band appears in the coordinant solvent, acetonitrile, while when the solvent has noncoordinant abilities, such as in dichloromethane, two bands appear, one at high energy and one at low energy, but with two exceptions, complexes **3** and **6**, in which in both solvents only the high energy band appears (see Table 4).

The high energy emissions are not likely to be due to metal-(gold or copper) centered transitions, usually appearing at lower energies.[21−24] This assumption, together with the fact that the pyrimidine ligand shows an emission at 369 nm (exc. 314 nm) in acetonitrile, prompted us to tentatively assign these emissions as mostly intraligand transitions, probably between π and π^* orbitals in the pyrimidine ligand. Nevertheless, the shifts in energy of this band between the different complexes indicate the participation of orbitals of the different ligands (nitriles and/or perhalophenyl groups) in the excited states. By contrast, the low energy emissions that appear only when the solvent used is dichloromethane appears at fairly similar energies to those in the solid state, suggesting a similar origin. In that sense, the assignment of this low energy band is not univocal, since there are several possibilities, for instance, metal-centered (MC), metal (gold or copper) to ligand (pyrimidine or nitrile) charge transfer (MLCT), or even intraligand (IL) or ligand to ligand charge transfer (LLCT). From these possibilities, both involving only ligands, it is highly unlikely due to the relatively low energy of the emissions. In addition, taking into account that, for Cu(I)-containing complexes with nitrogen donor ligands, the most common transition is the metal to ligand charge transfer, we propose that the emissions observed in the solid state, as well at low energies in dichloromethane, arise from a ^{3}(MLCT) state. This assignment is in accordance with the quenching of the low energy bands observed in acetonitrile solutions, whose emission spectra only display the high energy band attributed to transitions in the pyrimidine ligand.

The quenching is likely to occur via exciplex formation. As has been reported in complexes of the type $Cu(NN)_2^+$, for example, $Cu(dmp)_2^+$ (dmp = 2,9-dimethyl-1,10-phenantroline),

dx.doi.org/10.1021/ic102550z |*Inorg. Chem.* 2011, 50, 6910–6921

Scheme 2. Quenching Mechanism Promoted by Solvents with Donor Characteristics

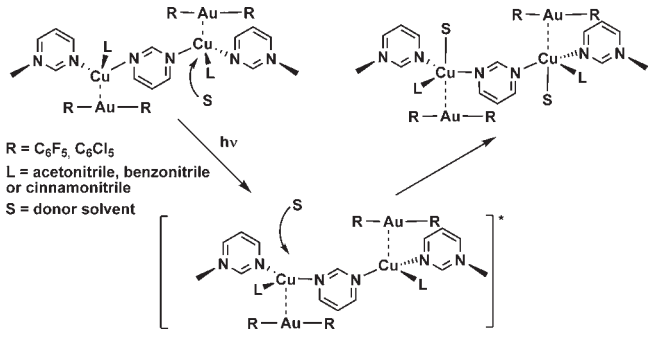

the emissions in dichloromethane are attributed to MLCT excited states, but the presence in the medium of nitrobenzene derivatives quenches those emissions via formation of encounter complexes without electron transfer.[25] Also, counterions with donor characteristics in these systems showed a quenching effect, which is stronger as the donor strength of the anion is bigger.[26] Solvents, being Lewis bases, also have the same effect.[27,28]

In those, as in this case, the quenching mechanism involves an associative attack by the solvent. Thus, if the copper centers are in the origin of the electronic transitions, the charge transfer excitation entails a formal increase in the oxidation state of these atoms. Specifically, the development of the Cu(II) character in the excited state provokes a flattening distortion, allowing the formation of five-coordinate adducts with a coordinate covalent bond between the copper center and the Lewis base acetonitrile (see Scheme 2). In fact, copper(II) compounds are frequently five-coordinate. Coordination of a fifth ligand stabilizes the charge transfer state and destabilizes the ground state, which promotes quenching[29,30] (Scheme 2).

In the case of dichloromethane solutions, the poor donor characteristics of this solvent prevent the formation of the five-coordinate complex, and therefore, the emission is not quenched. In the case of complexes **3** and **6**, with the cinnamonitrile ligand, this low energy emission is not detected in the solid state or in dichloromethane solution, but as we have commented, this fact could be related with a different charge transfer state, probably involving cinnamonitrile orbitals, that relaxes nonradiatively to the ground state (see Theoretical Calculations section).

On the other hand, it seems surprising that these LMCT states give rise to strong luminescences and long lifetimes when typically charge transfer states of copper(I) lead to weak emissions and are short-lived (nanoseconds range). Nevertheless, the reason for this behavior could be related to the presence in the complexes of strong donor groups $[Au(C_6X_5)_2]^-$, whose inductive effect by the interaction with the copper centers favors the copper to pyrimidine charge transfer transition.

Finally, from all of the complexes displaying low energy emission in the solid state, complex **5** shows an emission considerably shifted to red if it is compared to the others, which appear at fairly the same energy. Taking into account that, in this complex, in the solid state structure, $\pi-\pi$ interactions between the pentachlorophenyl and pyrimidine rings appear, we propose that the emission in this complex arises from an admixture of MLCT and $\pi(C_6Cl_5)-\pi$(pyrimidine) excited states.

Theoretical Calculations. In view of the interesting photophysical properties that these types of Au−Cu compounds display we have carried out DFT calculations on different bimetallic model systems. The aim of these calculations is to find a plausible explanation for the different behaviors observed for the complexes bearing the acetonitrile (**1**, **4**) or benzonitrile (**2**, **5**) ligands, which are luminescent in the solid state, and the cinnamonitrile ligand (**3**, **6**), which are not luminescent under the same conditions. We have chosen the DFT level of theory because it is less time-consuming than MP2 or higher correlated methods, which permits an analysis of the large models, and because the description of the Au···Cu interaction can be afforded within this level of theory since a high percentage of the ionic component (ca. 80%) is on the origin of this type of metallophilic Au···Cu interaction, as has been previously studied for other metal systems.[4d,5,31] We have carried out the full optimization of the ground (S_0) and the lowest triplet excited state (T_1), from which the phosphorescent emission occurs for dinuclear model systems of the type $[Au(C_6F_5)_2][Cu(L)(\mu_2\text{-}C_4H_4N_2)]$ (L = N≡C−Me, **1a**; N≡C−Ph, **2a**; N≡C−CH═CH−Ph, **3a**) in C_2 symmetry (see Figure 7 for a summary and Table 5). This type of theoretical approach permits one, first, to analyze the structural distortion of the molecules when they change from the ground to the first triplet excited state, relaying very important information on the photophysical properties. Second, we can analyze the shape of the frontier orbitals involved both in the ground (HOMO−LUMO) and in the lowest triplet state (SOMO−SOMO−1), which shows the parts of the molecule involved in the electronic transition (HOMO−SOMO) responsible for the phosphorescent behavior of these systems.

Table 5 displays selected X-ray bond distances and angles for complexes **1** and **3** and for DFT-B3LYP optimized models **1a**−**3a** in the ground state. The first result of these theoretical optimizations is that the obtained theoretical structural parameters are similar to the experimental ones obtained from X-ray diffraction studies, including the metallophilic interaction between Au(I) and Cu(I) centers.

The experimental lifetimes of the emissions of complexes **1** and **2** and complexes **4** and **5** in the microsecond range, suggesting phosphorescent processes, prompted us to optimize the lowest triplet excited states of models **1a**−**3a**. As we have mentioned above, with these optimizations, we can analyze the structural distortion and the orbitals involved in the phosphorescent emission of complexes **1** and **2** and complexes **4** and **5** and in the absence of phosphorescence in the case of complexes **3** and **6**. Regarding the structural distortions, Table 5 shows the most important optimized distances and angles of models **1a**−**3a** in the T_1 excited state. If we have a look at the results obtained for model system $[Au(C_6F_5)_2][Cu(N{\equiv}C{-}Me)(\mu_2\text{-}C_4H_4N_2)]$, **1a**, in the T_1 state and we compare it with the optimized structure in the S_0 ground state, we detect significant changes. Thus, we observe a shortening of the Au−Cu distance from 2.907 Å (S_0) to 2.564 Å (T_1) and, in a similar way, a shortening of ca. 0.1 Å in the Cu−pyrimidine distance. Nonetheless, an increase of the Cu−nitrile distance up to 2.222 Å is observed in the T_1 state with respect to the one observed in the ground state (S_0), 2.009 A (Figure 8). Also, the coordination environment of the Cu(I) center seems to be affected in the $S_0 \rightarrow T_1$ transition going from a pseudotetrahedral disposition in the ground state to an almost trigonal pyramidal arrangement. In fact, this distortion of the Cu(I) environment is in agreement with the proposed situation needed for the quenching mechanism in the presence of donor solvents for which a flattening distortion at Cu(I) and an associative attack by the solvent are proposed (see above).

In the same way as for model **1a**, model **2a** displays a very similar type of distortion in the lowest triplet excited state,

dx.doi.org/10.1021/ic102550z |Inorg. Chem. 2011, 50, 6910–6921

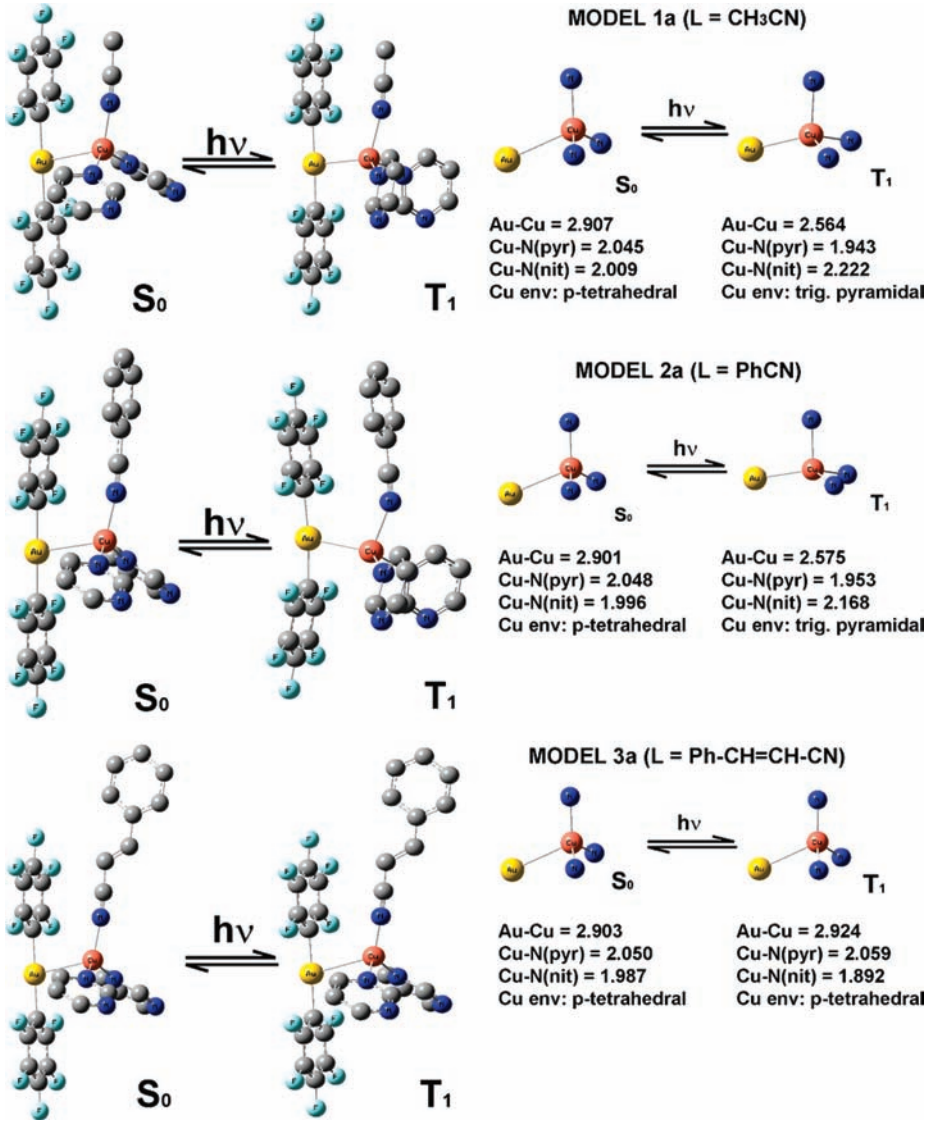

Figure 7. Optimized structures of the ground and lowest triplet excited states for models **1a**−**3a**.

i.e., metal−metal and copper−pryimidine distance shortening, a copper−nitrile distance increase, and flattening of the copper(I) environment, in agreement with a similar type of phosphorescent process for both types of complexes (see Table 5).

In principle, the surprising absence of a phosphorescent emission for complexes **3** and **6** bearing the cinnamonitrile ligand is reflected in a completely different distortion of model system **3a** when going from the ground to the first triplet excited state. Thus, in this case, both the Au−Cu and the Cu−pyrimidine distances remain almost unaffected, displaying a very slight enlargement compared to the ground state (see Table 5). The most striking feature in this case is that, instead of a separation of the nitrile ligand from the copper center, the cinnamonitrile ligand is closer to the heterometal in the excited state (1.892 Å in the T_1 state versus 1.987 Å in the S_0 state), which suggests a completely different excitation mechanism that would be related with a nonradiative decay, since the experimental measurements show the absence of phosphorescence for these Au−Cu complexes with the electron acceptor cinnamonitrile ligand. Indeed, if one observes carefully the structure of the cinnamonitrile ligand in the lowest triplet excited state of model system **3a**, it is clear that the $S_0 \rightarrow T_1$ transition arrives to a π^* orbital (see below), leading to an increase of the C−C distance of the double bond in the excited state. This trend would be related to a previously described twisting double bond[17] in a nonradiative decay pathway with a low-energy barrier that could be responsible for the absence of luminescence in the case of Au(I)−Cu(I) complexes **3** and **6**, bearing the cinnamonitrile ligand (Figure 9).

Another interesting result that can be derived from the full optimization of the S_0 and T_1 excited states is the analysis of the frontier molecular orbitals for each model systems. In general, we can attribute the HOMO (doubly highest occupied molecular orbital in the S_0 state) → SOMO (singly occupied molecular orbital in the T_1 state) transition as the origin for the photoluminescent properties of the complexes with acetonitrile or benzonitrile ligands or the nonradiative decay for complexes bearing the cinnamonitrile ligand. If we inspect carefully the shape of these orbitals for models **1a** and **2a**, we observe a similar situation. The HOMO orbital is mostly located at the bis(pentafluorophenyl)aurate units and at the Cu(I) centers, while

dx.doi.org/10.1021/ic102550z |*Inorg. Chem.* 2011, 50, 6910–6921

Table 5. Selected Experimental and Theoretical Distances (Å) and Angles (deg) for Complexes 1−3 and for Model Systems 1a−3a in the Ground (S_0) and Lowest Triplet Excited State (T_1)

	Au−Cu	Au−C	Cu−N_{py}	Cu−N_{CN}	C−Au-C	N_{CN}−Cu−N_{CN}	N_{Py}−Cu−N_{Py}	Au−Cu−N_{Py}	Au−Cu−N_{CN}
$\{[Au(C_6F_5)_2][Cu(N{\equiv}C-Me)(\mu_2\text{-}C_4H_4N_2)]\}_n$ (**1**)	2.821	2.045, 2.056	1.987, 2.003	2.048	178.09	97.74, 110.60	133.47	92.70, 91.37	135.95
$[Au(C_6F_5)_2][Cu(N{\equiv}C-Me)(\mu_2\text{-}C_4H_4N_2)]$ (**1a**), S_0	2.907	2.069, 2.072	2.045	2.009	179.97	112.09	125.89	94.88	113.39
$[Au(C_6F_5)_2][Cu(N{\equiv}C-Me)(\mu_2\text{-}C_4H_4N_2)]$ (**1a**), T_1	2.564	2.068	1.943	2.222	178.65	103.69	98.64	119.13	110.39
$[Au(C_6F_5)_2][Cu(N{\equiv}C-Ph)(\mu_2\text{-}C_4H_4N_2)]$ (**2a**), S_0	2.901	2.068, 2.072	2.048	1.996	179.97	112.31	125.73	94.97	113.39
$[Au(C_6F_5)_2][Cu(N{\equiv}C-Ph)(\mu_2\text{-}C_4H_4N_2)]$ (**2a**), T_1	2.575	2.071	1.953	2.168	174.60	103.50	98.97	125.18	98.99
$\{[Au(C_6F_5)_2][Cu(N{\equiv}C-CH{=}CH-Ph)(\mu_2\text{-}C_4H_4N_2)]\}_n$ (**3**)	2.761	2.047, 2.057	1.997, 2.001	2.000	176.58	109.71, 101.99	128.94	94.69, 95.52	128.67
$[Au(C_6F_5)_2][Cu(N{\equiv}C-CH{=}CH-Ph)(\mu_2\text{-}C_4H_4N_2)]$ (**3a**), S_0	2.903	2.069, 2.072	2.050	1.987	179.82	112.33	125.06	94.82	114.05
$[Au(C_6F_5)_2][Cu(N{\equiv}C-CH{=}CH-Ph)(\mu_2\text{-}C_4H_4N_2)]$ (**3a**), T_1	2.924	2.068	2.059	1.892	179.24	117.42	115.16	92.08	116.91

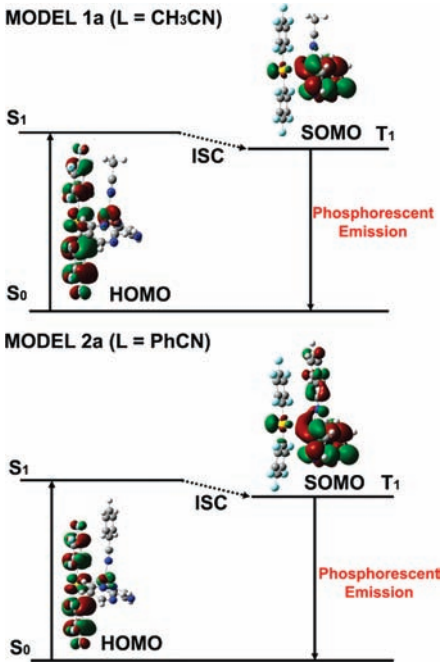

Figure 8. Molecular orbital diagrams displaying the highest occupied molecular orbital (HOMO) and highest singly occupied molecular orbital (SOMO) for model systems **1a** and **2a**.

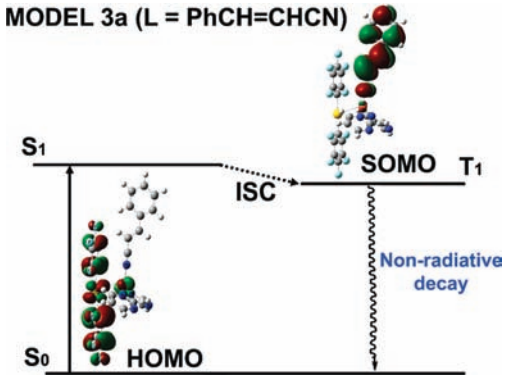

Figure 9. Molecular orbital diagram displaying the highest occupied molecular orbital (HOMO) and highest singly occupied molecular orbital (SOMO) for model system **3a**.

the SOMO orbital is mainly placed in both cases at the pyrimidine ligand (with some contribution of the nitrile in the case of benzonitrile). Therefore, taking into account the optimized structural distortions, the shape of the HOMO and SOMO orbitals, and the experimental results, we suggest that the origin of the phosphorescence for complexes **1**, **2**, **4**, and **5** is a charge transfer from the electron rich metals to the pyrimidine ligand ^{3}(MLCT) (Figure 8).

If we carry out a similar orbital analysis for HOMO and SOMO orbitals of model system $[Au(C_6F_5)_2][Cu(N{\equiv}C-CH{=}CH-Ph)(\mu_2\text{-}C_4H_4N_2)]$ (**3a**), we observe a different situation, that is also related to the different structural distortion of the lowest triplet excited state. As we have commented above, it seems that the structural changes mainly affect the cinnamonitrile ligand. In fact, while the HOMO orbital is very similar to the ones observed for models **1a** and **2a**, i.e., mostly located at the perhalophenyl ligands

Table 6. Natural Bond Orbital (NBO) Charge Transfer Distribution in the Different Molecular Components of Model Systems 1a−3a

component	1a (S_0)	1a (T_1)	2a (S_0)	2a (T_1)	3a (S_0)	3a (T_1)
Au	0.334	0.403	0.340	0.415	0.278	0.346
Cu	0.781	1.192	0.801	1.236	0.788	0.982
C_6F_5	−1.224	−1.200	−1.231	−1.208	−1.223	−1.231
pyrimidine	0.09	−0.427	0.084	−0.386	0.090	0.130
nitrile	0.02	0.038	0.011	−0.063	0.003	−0.233

and the metal centers, the SOMO orbital is now an antibonding orbital located at the cinnamonitrile ligand. This result and the structural distortion of the T_1 state support a different origin of the $S_0 \rightarrow T_1$ transition, and a nonradiative decay via a possible twisting of the C=C bond of the cinnamonitrile ligand is more likely (Figure 9).

In order to check that the assignment of the $S_0 \rightarrow T_1$ transitions is correct in terms of charge transfer processes, we have also carried out a NBO (natural bond orbital) analysis of the DFT density of the three model systems. As can be observed in Table 6, the charge distribution of the different molecular components is displayed both for the S_0 and for the T_1 states. Model systems **1a** and **2a** show that, in the ground state S_0, most of the electron density is placed at the formally monoanionic pentafluorophenyl rings (−1.224 (**1a**) and −1.231 (**2a**)) and cationic Au(I) (0.334 (**1a**) and 0.340 (**2a**)) and Cu(I) (0.781 (**1a**) and 0.801 (**2a**)) metal centers, with the pyrimidine (0.09 (**1a**) and 0.084 (**2a**)) and nitrile (0.02 (**1a**) and 0.011 (**2a**)) ligands remaining in their neutral forms. Upon excitation of one electron to the lowest T_1 excited state, the $C_6F_5^-$ ligands and the metal centers, especially Cu(I), lose part of their electron density that is now placed, through a charge transfer transition, mainly at the pyrimidine ligand (−0.427 (**1a**) and −0.386 (**2a**)), following the same trend seen in the structural distortion and the SOMO location for **1a** and **2a** model systems. Nevertheless, although the electron density for the ground state of model **3a** is also located at the bis(pentafluorophenyl)aurate unit and the copper(I) center, the electron density in the T_1 excited state is not placed at the pyrimidine but at the cinnamonitrile ligand, as we have previously commented upon.

We have also calculated the vertical transition from the T_1 to the S_0 state for the prediction of the emission energy for both phosphorescent systems with acetonitrile and benzonitrile ligands. We have chosen two different types of basis sets. The first one was the Andrae basis sets for Au, Dolg basis sets for Cu, and SVP for the rest of the atoms (two f polarization functions for the metals), and the second one was Andrae basis sets for Au, Dolg basis sets for Cu, and Stuttgart basis sets for the rest of the atoms (two f polarization functions for the metals and one d polarization function for the rest of atoms). In the first case, we have estimated a phosphorescent emission of 666 nm (525 nm exp in solid at RT) for complex **1** and 586 nm (522 nm exp in solid at RT) for complex **2**. If we change the quality to better basis sets for the nonmetallic atoms, the result is closer to the experimental one, being 530 nm (525 nm exp in solid at RT) for complex **1** and 544 nm (522 nm exp in solid at RT) for complex **2**.

In conclusion, we can state that, first, in charge transfer transitions in heteropolynuclear perhalophenyl−Au−Cu−nitrile complexes, the change of the perhalophenyl ligand bonded to gold(I) or the type of nitrile ligands bonded to Cu(I) permit a tuning of the emission energies by the modification of the basicity of the aurate units or the accepting abilities of the nitrile ligands. Second, when the nitrile ligand is cinnamonitrile, the charge transfer mechanism changes, promoting a nonradiative decay of the emission. Finally, the emission properties of the luminescent complexes in solution are strongly dependent on the donor characteristics of the solvents used. Thus, in donor solvents, the charge transfer excitation promotes a distortion in the excited state that allows the formation of a nonemitting five-coordinate adduct.

EXPERIMENTAL SECTION

General. The compounds $[\{AuAg(C_6F_5)_2(N{\equiv}C{-}Me)\}_2]_n$[15] and $\{[Au(C_6F_5)_2][Cu(N{\equiv}C{-}Me)(\mu_2\text{-}C_4H_4N_2)]\}_n$ (**1**)[8] were synthesized according to published procedures. Complex $[\{AuAg(C_6Cl_5)_2(N{\equiv}C{-}Me)\}_2]_n$ was prepared similarly to the analogous ones with pentafluorophenyl ligands by changing the aurate precursor. Solvents (spectroscopic grade) used in the spectroscopic studies were degassed prior to use.

Instrumentation. Infrared spectra were recorded in the 4000−200 cm^{-1} range on a Perkin-Elmer FT-IR Spectrum 1000 spectrophotometer, using Nujol mulls between polyethylene sheets. C, H, and N analyses were carried out with a C.E. Instrument EA-1110 CHNS-O microanalyzer. Mass spectra were recorded on a HP-5989B Mass Spectrometer API-Electrospray with interface 59987A. ^1H and ^{19}F NMR spectra were recorded on a Bruker ARX 300 in CD_3CN. Chemical shifts are quoted relative to $SiMe_4$ (^1H external) and $CFCl_3$ (^{19}F, external). Absorption spectra in solution were registered on a Hewlett-Packard 8453 Diode Array UV−visible spectrophotometer. Excitation emission spectra as well as lifetime measurements were recorded with a Jobin-Yvon Horiba Fluorolog 3−22 Tau-3 spectrofluorimeter.

Preparation of $\{[Au(C_6F_5)_2][Cu(N{\equiv}C\text{-}Ph)(\mu_2\text{-}C_4H_4N_2)]\}_n$ (2). To an acetonitrile solution (20 mL) of $[\{AuAg(C_6F_5)_2(N{\equiv}C{-}Me)\}_2]_n$ (111 mg, 0.156 mmol) was added CuCl (15 mg, 0.156 mmol), and a white precipitate was observed (AgCl). The mixture was stirred for 2 h, and the solid was eliminated by filtration. The solvent was removed by evaporation until dryness, leading to an orange solid. Toluene (20 mL) was added as a solvent, and benzonitrile (16 μL, 0.156 mmol) and pyrimidine (13 μL, 0.156 mmol) were added to the mixture. It was stirred for 20 min, and a white precipitate was observed. The solvent was evaporated to *ca.* 5 mL, and the addition of *n*-hexane (20 mL) led to complex **2** as a white solid. Yield: 73%. Elemental analysis (%) calcd. for **2** ($C_{23}H_9AuCuF_{10}N_3$): C, 35.51; H, 1.17; N, 5.40. Found: C, 35.40; H, 0.91; N, 5.37. ^{19}F (298 K, CD_3CN): δ −162.86 (m, 2F, F_m), −161.67 (t, 1F, F_p, $J_{Fo\text{-}Fp}$ = 19.3 Hz), −114.87 (m, 2F, F_o) ppm. ^1H (298 K, CD_3CN), benzonitrile ligand: δ 7.49 (m, 2H, H_1), 7.45 (m, 1H, H_3), 7.31 (m, 2H, H_2) ppm. ^1H (298 K, CD_3CN), pyrimidine ligand: δ 8.91 (s, 1H, H_1), 8.50 (m, 2H, H_2), 7.19 (m, 1H, H_3) ppm. MS (MALDI-): *m/z* 530.983 $[Au(C_6F_5)_2]^-$, 1124.862 $[Au_2Cu(C_6F_5)_4]^-$. FT-IR (Nujol mulls): ν 2240 cm^{-1} (C≡N), ν 1633−1564 cm^{-1} (C=N), ν 1502, 958, 785 cm^{-1} $[Au(C_6F_5)_2]$.

Preparation of $\{[Au(C_6F_5)_2][Cu(N{\equiv}C{-}CH{=}CH{-}Ph)(\mu_2\text{-}C_4H_4N_2)]\}_n$ (3). To an acetonitrile solution (20 mL) of $[\{AuAg(C_6F_5)_2(N{\equiv}C{-}Me)\}_2]_n$ (111 mg, 0.156 mmol) was added CuCl (15 mg, 0.156 mmol), and a white precipitate was observed (AgCl). The mixture was stirred for 2 h, and the solid was eliminated by filtration. The solvent was removed by evaporation until dryness, leading to an orange solid. Toluene (20 mL) was added as a solvent, and cinamonitrile (20 μL, 0.156 mmol) and pyrimidine (13 μL, 0.156 mmol) were added to the mixture. After 20 min of stirring, the solution turned light yellow, and a precipitate started to appear. The solvent was evaporated to *ca.* 5 mL, and the addition of *n*-hexane led to a light yellow solid. Yield: 75%. Crystals suitable for X-ray diffraction studies on **3** were obtained by slow diffusion of *n*-hexane into a concentrated solution of the complex in toluene. Elemental analysis (%) calcd. for **3** ($C_{25}H_{11}AuCuF_{10}N_3$): C, 37.35; H, 1.38; N, 5.23. Found: C, 37.26; H, 1.25; N, 4.97. ^{19}F (298 K, CD_3CN): δ −162.87 (m, 2F, F_m), −161.68 (t, 1F, F_p, $J_{Fo\text{-}Fp}$ = 19.4 Hz), −114.86 (m, 2F, F_o) ppm. ^1H

dx.doi.org/10.1021/ic102550z |*Inorg. Chem.* 2011, 50, 6910–6921

(298 K, CD_3CN), cinnamonitrile ligand: δ 5.87 (d, 1H, H_3, $^3J_{CH=CH}$ = 13.0 Hz), 7.26 [(m, 1H, H_2), (m, 5H, H_1)] ppm. ^1H (298 K, CD_3CN), pyrimidine ligand: δ 8.92 (s, 1H, H_1), 8.51 (m, 2H, H_2), 7.26 (m, 1H, H_3) ppm. MS (MALDI−): m/z 530.887 $[Au(C_6F_5)_2]^-$, 760.782 $[AuCu(C_6F_5)_3]^-$, 1124.681 $[Au_2Cu(C_6F_5)_4]^-$. MALDI(+) m/z: 272.060 $[Cu(N{\equiv}C-CH{=}CH-Ph)(C_4H_4N_2)]^+$, 321.097 $[Cu(N{\equiv}C-CH{=}CH-Ph)_2]^+$. FT-IR (Nujol mulls): ν 2235 cm^{-1} (C≡N), ν 1633−1577 cm^{-1} (C═N), ν 1499, 955, 785 cm^{-1} $[Au(C_6F_5)_2]$.

Preparation of $\{[Au(C_6Cl_5)_2][Cu(N{\equiv}C-Me)(\mu_2\text{-}C_4H_4N_2)]\}_n$ (4). To an acetonitrile solution (20 mL) of $[\{AuAg(C_6Cl_5)_2(N{\equiv}C-Me)\}_2]_n$ (95 mg, 0.112 mmol) was added CuCl (11 mg, 0.112 mmol), and a white precipitate was observed (AgCl). The mixture was stirred for 2 h, and the solid was eliminated by filtration. The filtrated solvent was evaporated to dryness, and a white solid was obtained. This solid was treated with toluene (20 mL), giving rise to a white suspension, and pyrimidine (8.82 μL, 0.112 mmol) was added, leading to a yellow solution. The mixture was stirred for 1 h, and after this time the solvent was evaporated to dryness, obtaining complex **4** as a white solid. Yield: 77%. Elemental analysis (%) calcd. for **4** ($C_{18}H_7AuCuCl_{10}N_3$): C, 24.56; H, 0.80; N, 4.77. Found: C, 24.61; H, 1.01; N, 4.75. ^1H acetonitrile ligand (298 K, $CDCl_3$): 2.10 (s, 3H, CH_3) ppm. ^1H pyrimidine ligand (298 K, CD_3CN) δ: 8.91 ppm (m, 1H, H_1), 8.52 ppm (m, 2H, H_2), 7.20 ppm (m, 1H, H_3). MS (MALDI+): m/z 184.096 $[Cu(N{\equiv}C-Me)(C_4H_4N_2)]^+$. MS (MALDI−): m/z 694.544 $[Au(C_6Cl_5)_2]^-$, 1455.993 $[Au_2Cu(C_6Cl_5)_4]^-$. FT-IR (Nujol mulls): ν 2273 cm^{-1} (C≡N), ν 1586−1560 cm^{-1} (C═N), ν 835, 609 cm^{-1} $[Au(C_6Cl_5)_2]$.

Preparation of $\{[Au(C_6Cl_5)_2][Cu(N{\equiv}C\text{-}Ph)(\mu_2\text{-}C_4H_4N_2)]\}_n$ (5). To an acetonitrile solution (20 mL) of $[\{AuAg(C_6Cl_5)_2(N{\equiv}C-Me)\}_2]_n$ (95 mg, 0.112 mmol) was added CuCl (11 mg, 0.112 mmol), and a white precipitate was formed (AgCl). The mixture was stirred for 2 h, and the solid was eliminated by filtration. The solvent was evaporated to dryness, and a white solid was obtained. This solid was treated with toluene (20 mL), giving rise to a white suspension. Benzonitrile (11.5 μL, 0.112 mmol) and pyrimidine (8.82 μL, 0.112 mmol) were added, leading to a yellow solution. A few seconds later, a yellow precipitate started to appear, and the mixture was stirred for 2 h. The solvent was evaporated to *ca.* 5 mL, and the addition of *n*-hexane led to the precipitation of complex **5** as a yellow solid. Yield: 69%. Crystals suitable for X-ray diffraction studies on **5** were obtained by slow diffusion of *n*-hexane into a concentrated solution of the complex in toluene. Elemental analysis (%) calcd. for **5** ($C_{23}H_9AuCuCl_{10}N_3$): C, 29.31; H, 0.96; N, 4.46. Found: C, 29.50; H, 1.20; N, 4.49. ^1H (298 K, CD_3CN), acetonitrile ligand: 7.50 ppm (m, 2H, H_1), 7.44 ppm (m, 1H, H_3), 7.31 ppm (m, 2H, H_2). ^1H (298 K, CD_3CN), pyrimidine ligand: δ 8.92 ppm (m, 1H, H_1), 8.52 ppm (m, 2H, H_2), 7.19 ppm (m, 1H, H_3). MS (MALDI+): m/z 184. 246.065 $[Cu(N{\equiv}C-Ph)(C_4H_4N_2)]^+$. MS (MALDI−): m/z 694.618 $[Au(C_6Cl_5)_2]^-$, 1454.161 $[Au_2Cu(C_6Cl_5)_4]^-$. FT-IR (Nujol mulls): ν 2245 cm^{-1} (C≡N), ν 1598−1561 cm^{-1} (C═N), ν 834, 612 cm^{-1} $[Au(C_6Cl_5)_2]$.

Preparation of $\{[Au(C_6Cl_5)_2][Cu(N{\equiv}C-CH{=}CH-Ph)(\mu_2\text{-}C_4H_4N_2)]\}_n$ (6). To an acetonitrile solution (20 mL) of $[\{AuAg(C_6Cl_5)_2(N{\equiv}C-Me)\}_2]_n$ (95 mg, 0.112 mmol) was added CuCl (11 mg, 0.112 mmol), and a white precipitate was observed (AgCl). The mixture was stirred for 2 h, and the solid was eliminated by filtration. The solvent was evaporated to dryness, and a white solid was obtained. This solid was treated with toluene (20 mL), giving rise to a white suspension; then cinnamonitrile (14.3 μL, 0.112 mmol) and pyrimidine (8.82 μL, 0.112 mmol) were added, leading to a yellow solution. A few seconds later, a yellow precipitate started to appear, and the mixture was stirred for 2 h. The solvent was evaporated to *ca.* 5 mL, and the addition of *n*-hexane led to the precipitation of complex **6** as a yellow solid. Yield: 56%. Elemental analysis (%) calcd. for **6** ($C_{25}H_{11}AuCuCl_{10}N_3$): C, 31.00; H, 1.14; N, 4.34. Found: C, 31.11; H, 1.32; N, 4.56. ^1H (298 K, CD_3CN), cinnamonitrile ligand: 7.26−7.35 ppm (m, 5H, H_1 and m, 1H, H_2), 5.90 ppm (d, 1H, H_3, $^3J_{CH=CH}$ = 13.0 Hz). ^1H (298 K, CD_3CN), pyrimidine ligand: δ 8.95 ppm (s, 1H, H_1), 8.54 ppm (m, 2H, H_2), 7.26−7.35 ppm (m, 1H, H_3). MS (MALDI+): m/z 0.988 $[Cu(N{\equiv}C-CH{=}CH-Ph)(C_4H_4N_2)]^+$, $[Cu(N{\equiv}C-CH{=}CH-Ph)_2]^+$. MS (MALDI−): m/z 694.553 $[Au(C_6Cl_5)_2]^-$, 1454.074 $[Au_2Cu(C_6Cl_5)_4]^-$. FT-IR (Nujol mulls): ν 2228 cm^{-1} (C≡N), ν 1612−1559 cm^{-1} (C═N), ν 833, 610 cm^{-1} $[Au(C_6Cl_5)_2]$.

Crystallography. Single crystals of **3** and **5** were mounted in mineral oil on a glass fiber and transferred to the cold stream of a Nonius Kappa CCD diffractometer equipped with an Oxford Instruments low-temperature attachment. Data were collected using monochromated Mo Kα radiation (λ = 0.71073 Å) with scan types ω and ϕ and semiempirical absorption correction (based on multiple scans). The structures were solved by direct methods and refined on F^2 using SHELXL-97.[32] All non-hydrogen atoms were anisotropically refined, and hydrogen atoms were included using a riding model. Further details regarding the data collection and refinement methods are listed in Table 1. Selected bond lengths and angles are listed in Tables 2 and 3, and the crystal structures of **3** and **5** are shown in Figures 1−4. Crystallographic data for the structures reported in this paper have been deposited with the Cambridge Crystallographic Data Centre as supplementary publication nos. CCDC-803579 and CCDC-803580. Copies of the data can be obtained free of charge on application to CCDC, 12 Union Road, Cambridge CB2 1EZ, U.K. (fax: (0.44) 1223−336−033; e-mail: deposit@ccdc.cam.ac.uk).

Computational Details. All calculations were carried out using the Gaussian 03 software package.[33] The model systems used in the theoretical studies of $[Au(C_6F_5)_2][Cu(L)(\mu_2\text{-}C_4H_4N_2)]$ (L = N≡C−Me (**1a**), N≡C−CH═CH−Ph (**3a**)) were built up from the X-ray diffraction data for complexes **1** and **3**, respectively. In the case of model system $[Au(C_6F_5)_2][Cu(L)(\mu_2\text{-}C_4H_4N_2)]$ (L = N≡C−Ph (**2a**)), the acetonitrile ligand from model **1a** was replaced by a benzonitrile one. Full DFT optimizations were performed on the model systems in C_2 symmetry. In both the ground-state and the lowest triplet excited state calculations, the B3LYP functional[34] as implemented in Gaussian 03 was used. In most calculations, the Karlsruhe split-valence quality basis sets (SVP)[35] augmented with polarization functions[36] were used for the heteroatoms, and the 19-VE pseudopotentials from Stuttgart and the corresponding basis sets for Au[37] and Cu[38] augmented with two f polarization functions were used.[39] In the case of the emission energy estimation, atoms C, N, and F were treated by Stuttgart pseudopotentials,[40] including only the valence electrons for each atom. For these atoms, the double-ζ basis sets of ref 40 were used, augmented by d-type polarization functions.[41] For the H atom, a double-ζ plus a p-type polarization function was used.[42]

■ ASSOCIATED CONTENT

Supporting Information. X-ray crystallographic data in CIF format for **3** and **5**. This material is available free of charge via the Internet at http://pubs.acs.org.

■ AUTHOR INFORMATION

Corresponding Author

*E-mail: josemaria.lopez@unirioja.es.

■ ACKNOWLEDGMENT

The D.G.I. (MEC)/FEDER (CTQ2010-20500-C02-02) project is acknowledged for financial support. D.P. And M.R.-C. thank the Comunidad Autónoma de La Rioja for their grants.

■ REFERENCES

(1) (a) Pyykkö, P. *Chem. Rev.* **1997**, *97*, 597. (b) Pyykkö, P *Angew. Chem., Int. Ed.* **2004**, *43*, 4412. (c) Pyykkö, P. *Inorg. Chim. Acta* **2005**, *358*, 4113. (d) Pyykkö, P. *Chem. Soc. Rev.* **2008**, *37*, 1967.

(2) (a) Fernández, E. J.; Laguna, A.; López-de-Luzuriaga, J. M. *Dalton Trans* **2007**, 1969.(b) López-de-Luzuriaga, J. M. In *Modern Supramolecular Gold Chemistry*; Laguna, A., Ed.; Wiley-VCH: Weinheim, Germany, 2008;p 347.

(3) (a) Fernández, E. J.; Gimeno, M. C.; Laguna, A.; López-de-Luzuriaga, J. M.; Monge, M.; Pyykkö, P.; Sundholm, D. *J. Am. Chem. Soc.* **2000**, *122*, 7287. (b) Fernández, E. J.; López-de-Luzuriaga, J. M.; Monge, M.; Olmos, M. E.; Puelles, R. C.; Laguna, A.; Mohamed, A. A.; Fackler, J. P., Jr. *Inorg. Chem.* **2008**, *47*, 8069. (c) Fernández, E. J.; Jones, P. G.; Laguna, A.; López-de-Luzuriaga, J. M.; Monge, M.; Olmos, M. E.; Puelles, R. C. *Organometallics* **2007**, *26*, 5931. (d) Catalano, V. J.; Etogo, A. O. *J. Organomet. Chem.* **2005**, *690*, 6041.(e) Catalano, V. J.; Moore, A. L. (f) Catalano, V. J.; Malwitz, M. A.; Etogo, A. O. *Inorg. Chem.* **2004**, *43*, 5714. (f) Burini, A.; Fackler, J. P., Jr.; Galassi, R.; Pietroni, B. R.; Staples, R. J. *Chem. Commun.* **1998**, 95.

(4) (a) Fernández, E. J.; López-de-Luzuriaga, J. M.; Monge, M.; Olmos, M. E.; Pérez, J.; Laguna, A.; Mohamed, A. A.; Fackler, J. P., Jr. *J. Am. Chem. Soc.* **2003**, *125*, 2022. (b) Fernández, E. J.; Laguna, A.; López-de-Luzuriaga, J. M.; Monge, M.; Olmos, M. E.; Pérez, J. *J. Am. Chem. Soc.* **2002**, *124*, 5942. (c) Fernández, E. J.; López-de-Luzuriaga, J. M.; Monge, M.; Montiel, M.; Olmos, M. E.; Pérez, J.; Laguna, A.; Mendizabal, F.; Mohamed, A. A.; Fackler, J. P., Jr. *Inorg. Chem.* **2004**, *43*, 3573. (d) Fernández, E. J.; Laguna, A.; López de Luzuriaga, J. M.; Mendizabal, F.; Monge, M.; Olmos, M. E.; Pérez, J. *Chem.—Eur. J.* **2003**, *9*, 456. (e) Fernández, E. J.; Jones, P. G.; Laguna, A.; López-de-Luzuriaga, J. M.; Monge, M.; Olmos, M. E.; Pérez, J. *Inorg. Chem.* **2002**, *41*, 1056. (f) Catalano, V. J.; Bennett, B. L.; Kar, H. M. *J. Am. Chem. Soc.* **1999**, *121*, 10235. (g) Burini, A.; Bravi, R.; Fackler, J. P., Jr.; Galassi, R.; Grant, T. A.; Omary, M. A.; Pietroni, B. R.; Staples, R. J. *Inorg. Chem.* **2000**, *39*, 3158.

(5) Fernández, E. J.; Laguna, A.; López-de-Luzuriaga, J. M.; Monge, M.; Nema, M.; Olmos, M. E.; Pérez, J.; Silvestru, C. *Chem. Commun.* **2007**, 571.

(6) Burini, A.; Fackler, J. P., Jr.; Galassi, R.; Grant, T. A.; Omary, M. A.; Rawashdeh-Omary, M. A.; Pietroni, B. R.; Staples, R. J. *J. Am. Chem. Soc.* **2000**, *122*, 11264.

(7) Catalano, V. J.; Malwitz, M. A.; Noll, B. C. *Chem. Commun.* **2001**, 581.

(8) Fernández, E. J.; Laguna, A.; López-de-Luzuriaga, J. M.; Monge, M.; Montiel, M.; Olmos, M. E. *Inorg. Chem.* **2005**, *44*, 1163.

(9) Fernández, E. J.; Laguna, A.; López-de-Luzuriaga, J. M.; Monge, M.; Olmos, M. E.; Montiel, M. *Inorg. Chem.* **2007**, *46*, 2953.

(10) Crespo, O.; Fernández, E. J.; Jones, P. G.; Laguna, A.; López-de-Luzuriaga, J. M.; Mendía, A.; Monge, M.; Olmos, E. *Chem. Commun.* **1998**, 2233.

(11) Fernández, E. J.; Jones, P. G.; Laguna, A.; López-de-Luzuriaga, J. M.; Monge, M.; Pérez, J.; Olmos, M. E. *Inorg. Chem.* **2002**, *41*, 1056.

(12) Fernández, E. J.; Laguna, A.; López-de-Luzuriaga, J. M.; Olmos, M. E.; Pérez, J. *Dalton Trans.* **2004**, 1801.

(13) (a) Bauernschmitt, R.; Ahlrichs, R. *Chem. Phys. Lett.* **1996**, *256*, 454. (b) Bauernschmitt, R.; Ahlrichs, R. *J. Chem. Phys.* **1996**, *104*, 9047. (c) Bauernschmitt, R.; Häser, M.; Treutler, O.; Ahlrichs, R. *Chem. Phys. Lett.* **1997**, *264*, 573 and refs therein. (d) Gross, E. K. U.; Kohn, W. *Adv. Quant. Chem.* **1990**, *21*, 255.(e) Casida, M. E. In *Recent Advances in Density Functional Methods*; Chong, D. P., Eds.; World Scientific: River Edge, NJ, 1995; Vol 1. (f) Olsen, J.; Jørgensen, P. In *Modern Electronic Structure Theory*; Yarkony, D. R., Ed.; World Scientific: River Edge, NJ, 1995; Vol 2.

(14) Bojan, V. R.; Fernández, E. J.; Laguna, A.; López-de-Luzuriaga, J. M.; Monge, M.; Olmos, M. E.; Silvestru, C. *J. Am. Chem. Soc.* **2005**, *127*, 11564.

(15) Fernández, E. J.; Laguna, A.; López-de-Luzuriaga, J. M.; Monge, M.; Montiel, M.; Olmos, M. E.; Rodríguez-Castillo, M. *Organometallics* **2006**, *26*, 3639.

(16) Fernández, E. J.; Laguna, A.; López-de-Luzuriaga, J. M.; Monge, M.; Montiel, M.; Olmos, M. E.; Rodríguez-Castillo, M. *Dalton Trans.* **2009**, 7509.

(17) (a) Pan, Y.; Zhao, J.; Ji, Y.; Yan, L.; Yu, S. *Chem. Phys.* **2006**, *320*, 125. (b) Lewis, F. D.; Hougland, J. L.; Markarian, S. A. *J. Phys. Chem. A* **2000**, *104*, 3261.

(18) Fernández, E. J.; Laguna, A.; López-de-Luzuriaga, J. M.; Monge, M.; Montiel, M.; Olmos, M. E.; Rodríguez-Castillo, M. *Open Inorg. Chem. J.* **2008**, *2*, 73.

(19) Albano, V. G.; Castellari, C.; Femoni, C.; Iapalucci, M. C.; Longoni, G.; Monari, M.; Zacchini, S. *J. Cluster Sci.* **2001**, *12*, 75.

(20) Haupt, H.-J.; Seewald, O.; Florke, U.; Buss, V.; Weyhermuller, T. *J. Chem. Soc., Dalton Trans.* **2001**, 3329.

(21) Forward, J. M.; Fackler, J. P., Jr.; Assefa, Z. In *Optoelectronic Properties of Inorganic Compounds*; Roundhill, D. M., Fackler, J. P., Jr., Eds.; Plenum: New York, 1999; pp 195−226.

(22) Che, C.-M.; Mao, Z.; Mikowski, V. M.; Tse, M.-C.; Chan, C.-K.; Cheung, K.-K.; Phillips, D. L.; Leung, K.-H. *Angew. Chem., Int. Ed.* **2000**, *39*, 4084.

(23) Ford, P. C.; Cariati, E.; Bourassa, J. *Chem. Rev.* **1999**, *99*, 3625.

(24) See, for example: Simon, J. A.; Palke, W. E.; Ford, P. C. *Inorg. Chem.* **1996**, *35*, 6413.

(25) Blaskie, M. W.; McMillin, D. R. *Inorg. Chem.* **1980**, *19*, 3519.

(26) Everly, R. M.; McMillin, D. R. *Photochem. Photobiol.* **1989**, *50*, 711.

(27) Palmer, C. E. A.; McMillin, D. R.; Kirmaier, C.; Holten, D. *Inorg. Chem.* **1987**, *26*, 3167.

(28) Stacy, E. M.; McMillin, D. R. *Inorg. Chem.* **1990**, *29*, 393.

(29) McMillin, D. R.; McNett, K. M. *Chem. Rev.* **1998**, *98*, 1201.

(30) (a) Sakaki, S.; Mizutani, H.; Kase, Y. *Inorg. Chem.* **1992**, *31*, 4575. (b) Eggleston, M. K.; McMillin, D. R.; Koenig, K. S.; Pallenberg, J. A. *Inorg. Chem.* **1997**, *36*, 172. (c) Everly, R. M.; Ziesel, R.; Suffert, J.; McMillin, D. R. *Inorg. Chem.* **1991**, *30*, 559. (d) Shinozaki, K.; Kaizu, Y. *Bull. Chem. Soc. Jpn.* **1994**, *67*, 2435.

(31) Fernández, E. J.; Laguna, A.; López-de-Luzuriaga, J. M.; Monge, M.; Pyykkö, P.; Runeberg, N. *Eur. J. Inorg. Chem.* **2001**, 750.

(32) Sheldrick, G. M. *SHELXL-97*; University of Göttingen: Göttingen, Germany, 1997.

(33) Frisch, M. J.; Trucks, G. W.; Schlegel, H. B.; Scuseria, G. E.; Robb, M. A.; Cheeseman, J. R.; Montgomery, J. A., Jr.; Vreven, T.; Kudin, K. N.; Burant, J. C.; Millam, J. M.; Iyengar, S. S.; Tomasi, J.; Barone, V.; Mennucci, B.; Cossi, M.; Scalmani, G.; Rega, N.; Petersson, G. A.; Nakatsuji, H.; Hada, M.; Ehara, M.; Toyota, K.; Fukuda, R.; Hasegawa, J.; Ishida, M.; Nakajima, T.; Honda, Y.; Kitao, O.; Nakai, H.; Klene, M.; Li, X.; Knox, J. E.; Hratchian, H. P.; Cross, J. B.; Bakken, V.; Adamo, C.; Jaramillo, J.; Gomperts, R.; Stratmann, R. E.; Yazyev, O.; Austin, A. J.; Cammi, R.; Pomelli, C.; Ochterski, J. W.; Ayala, P. Y.; Morokuma, K.; Voth, G. A.; Salvador, P.; Dannenberg, J. J.; Zakrzewski, V. G.; Dapprich, S.; Daniels, A. D.; Strain, M. C.; Farkas, O.; Malick, D. K.; Rabuck, A. D.; Raghavachari, K.; Foresman, J. B.; Ortiz, J. V.; Cui, Q.; Baboul, A. G.; Clifford, S.; Cioslowski, J.; Stefanov, B. B.; Liu, G.; Liashenko, A.; Piskorz, P.; Komaromi, I.; Martin, R. L.; Fox, D. J.; Keith, T.; Al-Laham, M. A.; Peng, C. Y.; Nanayakkara, A.; Challacombe, M.; Gill, P. M. W.; Johnson, B.; Chen, W.; Wong, M. W.; Gonzalez, C.; Pople, J. A. *Gaussian 03*, Revision C.02; Gaussian, Inc.: Wallingford, CT, 2004.

(34) (a) Becke, A. D. *J. Chem. Phys.* **1992**, *96*, 215. (b) Becke, A. D. *J. Chem. Phys.* **1993**, *98*, 5648. (c) Lee, C.; Yang, W.; Parr, R. G. *Phys. Rev. Lett.* **1998**, *B 37*, 785.

(35) Schäfer, A.; Horn, H.; Ahlrichs, R. *J. Chem. Phys.* **1992**, *97*, 2571.

(36) Dunning, T. H., Jr. *J. Chem. Phys.* **1994**, *100*, 5829.

(37) Andrae, D.; Häusserman, U.; Dolg, M.; Stoll, H.; Preuss, H. *Theor. Chim. Acta* **1990**, *77*, 123.

(38) Dolg, M.; Wedig, U.; Stoll, H.; Preuss, H. *J. Chem. Phys.* **1987**, *86*, 866.

(39) Pyykkö, P.; Runeberg, N.; Mendizabal, F. *Chem.—Eur. J.* **1997**, *3*, 1451.

(40) Bergner, A.; Dolg, M.; Küchle, W.; Stoll, H.; Preuss, H. *Mol. Phys.* **1993**, *80*, 1431.

(41) Huzinaga, S. *Gaussian Basis Sets for Molecular Calculations*; Elsevier: Amsterdam, 1984; p 16.

(42) Huzinaga, S. *J. Chem. Phys.* **1965**, *42*, 1293.